



Title	Photonic ultrawideband pulse generation with HNL-DSF-based phase and intensity modulator
Author(s)	Zhou, E; Xu, X; Lui, KS; Wong, KKY
Citation	IEEE Photonics Technology Letters, 2011, v. 23 n. 7, p. 396-398
Issued Date	2011
URL	http://hdl.handle.net/10722/135110
Rights	IEEE Photonics Technology Letters. Copyright © IEEE.

Photonic Ultrawideband Pulse Generation With HNL-DSF-Based Phase and Intensity Modulator

Enbo Zhou, Xing Xu, *Student Member, IEEE*, K. S. Lui, and Kenneth K. Y. Wong, *Senior Member, IEEE*

Abstract—We propose and experimentally demonstrate a photonic ultrawideband (UWB) pulse (monocycle and doublet) generator based on a highly nonlinear dispersion-shifted fiber (HNL-DSF). The pulsed pump, located in the anomalous group-velocity dispersion regime of the HNL-DSF, performs as both an intensity and a phase modulator in our scheme. We experimentally prove, for the first time to the best of our knowledge, that the UWB doublet pulse can be generated when the optical carrier is located at the center of a narrow tunable filter's passband. Furthermore, the encoded doublet signal, fully compliant with the Federal Communications Commission (FCC) regulations, is transmitted at 950 Mb/s through a 25-km single-mode fiber without introducing any obvious pulse distortion.

Index Terms—Cross-phase modulation (XPM), microwave photonics, optical parametric amplifier (OPA), ultrawideband (UWB)-over-fiber.

I. INTRODUCTION

IMULSE radio based ultrawideband (UWB) communication systems have the advantages of high data rate transmission with extremely low radiation power, and potential low-cost operation due to the unlicensed frequency range from 3.1 to 10.6 GHz, specified by the Federal Communications Commission (FCC)[1]. However, with the low radiation power prescribed by FCC, the wireless operation range is limited to the immediate area (up to tens of meters). With the rapid development of radio-over-fiber (RoF) technologies, the transmission distance of UWB signals can be extended enormously through ordinary optical fiber. Furthermore, in order to reduce the complexity and achieve seamless interconnection among different network infrastructures, it is thus required to generate UWB signals directly in the optical domain [2]. Various solutions have recently been reported for UWB-over-fiber communication systems [2]–[14]. A widely-adopted technique is to convert red- and blue-shifted chirp to monocycle or doublet UWB pulses by locating the carrier wavelength at the linear or the quadrature slopes of a fiber Bragg grating (FBG) [2], [3]. However, the

tunability of the carrier wavelength is limited by the fixed reflected wavelength of FBGs. Moreover, using the concept of optical injection, optical systems, based on semiconductor optical amplifiers (SOAs) [4]–[6] and distributed feedback (DFB) lasers [7]–[9], can also generate UWB signals by direct intensity modulation. However, active device based schemes could be negatively impacted by the slow carrier response due to the band-filling effect [4]–[9]. While the highly-nonlinear dispersion-shifted fiber (HNL-DSF), with ultrafast response time inherited from the third-order susceptibility ($\chi^{(3)}$), has no such concern, and it shows great potential in generating distortion-free and high speed UWB pulses [14], [15]. On the modulation side, with switchable polarity and shape modulation, some modulation techniques including binary phase modulation (BPM), pulse shape modulation (PSM) are reported recently [10], [11]. However, such techniques require multiple wavelengths which may suffer potential problems in long distance transmission. Electrically reconfigurable multiple modulation formats may provide potential solution, only if the undesirable parasitic pulses, produced during the transient state of power switching, can be suppressed adequately to mitigate the signal distortion in transmission [12]. Whereas ON-OFF keying (OOK) modulated UWB signal with low complexity has enhanced peak-to-peak pulse power and gets more easily access across the metropolitan area network (MAN)[7], [13].

In this letter, we experimentally demonstrate the generation of UWB monocycle and doublet pulses by combination of optical parametric amplification (OPA) and cross-phase modulation (XPM) effect in the HNL-DSF. We experimentally prove that, for the first time as to the best of our knowledge, the UWB doublet pulses can be generated while the optical carrier is located at the center passband of an optical filter. Moreover, the pulse can be shaped to better comply with the FCC mask by balancing the effect of OPA and XPM on the probe wave. Comparing to the pure phase modulation to intensity modulation (PM-IM) conversion schemes [2], [3], which use the frequency discriminator with fixed wavelength once fabricated, the enhanced wavelength tunability and flexibility of pulse shaping can be achieved simultaneously in our scheme. Different from [14], the average pump power is enormously reduced nearly by 12-dB here due to the pulsed pump light. Furthermore, benefiting from one single wavelength operation, the encoded doublet signal, fully compliant with the FCC regulations, is transmitted at 950 Mb/s through 25 km single-mode fiber (SMF) without obvious pulse distortion.

II. PRINCIPLE AND EXPERIMENTAL SETUP

It is well-known that the rising and falling edges of the pump pulse will lead to red- and blue-shift on the probe beam due to XPM, respectively. Furthermore, a pulse pump, locating in the

Manuscript received November 17, 2010; revised December 17, 2010; accepted January 07, 2011. Date of publication January 17, 2011; date of current version March 11, 2011. This work was supported by grants from the Research Grants Council of the Hong Kong S.A.R., China (projects HKU7179/08E and 7183/09E), and by Sumitomo for the HNL-DSF and Alnair Laboratories for the VBTBPF.

E. Zhou is with Huawei Technologies Co., Ltd., Shenzhen 518000, China (e-mail: nbzhou@huawei.com).

X. Xu, K. S. Lui, and K. K. Y. Wong are with the Photonic Systems Research Laboratory, The Department of Electrical and Electronic Engineering, The University of Hong Kong, Hong Kong S.A.R., China (e-mail: xuxing@eee.hku.hk; kslui@eee.hku.hk; kywong@eee.hku.hk).

Color versions of one or more of the figures in this letter are available online at <http://ieeexplore.ieee.org>.

Digital Object Identifier 10.1109/LPT.2011.2106770

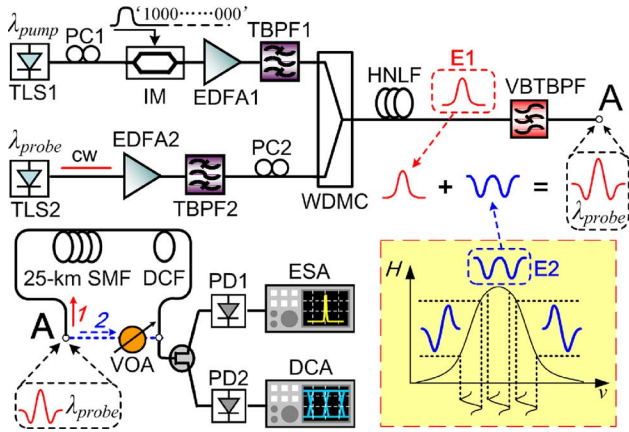


Fig. 1. Experimental setup of HNL-DSF-based UWB pulse generation system, with the inset (dashed box) illustrating the principle of phase modulation to temporal intensity modulation conversion.

anomalous group-velocity dispersion (GVD) regime near the zero-dispersion wavelength (ZDW) of the HNL-DSF, leads to intensity modulation due to OPA. In the pump-probe scheme, the OPA gain and 3-dB gain bandwidth are very sensitive to the pump wavelength. Due to the different responses of XPM and OPA to pump wavelength variation, the pump wavelength selection is critical to balance the XPM and OPA effects on the probe wave. The contribution of OPA increases exponentially when the difference between pump wavelength and ZDW of the HNL-DSF decreases. In contrast, if the pump wavelength moves far away from the ZDW, the gain bandwidth of OPA decreases dramatically. However, the XPM was not influenced obviously while pump power maintains the same. In this case, an optimal pump wavelength was selected once a compromise between a moderate OPA gain and the PM-IM conversion reaches. The inset dashed box of Fig. 1 illustrates the principle of PM-IM conversion. When the probe wavelength locates at either side of the linear slopes of the transmission function (H) of the variable bandwidth tunable bandpass filter (VBTBPF), the XPM dominates due to the fact that the probe light is filtered by the detuned VBTBPF. As a result, through PM-IM conversion, a pair of monocycle UWB pulses with inverted polarities can be generated alternatively [3]. However, if the probe wave is located at the central wavelength of the VBTBPF, the OPA effect cannot be omitted. On one hand, a pulse-like probe waveform with continuous wave (CW) pedestal is induced due to OPA effect (E1 in Fig. 1). In our experiment, the measured average OPA gain G_a is 3-dB. And the duty ratio D_r of the pulsed pump is 1/30, thus the peak gain G_p is 14.8-dB, from the following equation [16]:

$$G_p = 10 \log \left(10^{G_a/10} \times \frac{1}{D_r} - \frac{1 - D_r}{D_r} \right). \quad (1)$$

On the other hand, due to symmetric PM-IM conversion, a symmetric intensity conversion from red- and blue-shifted frequency chirp will be introduced (E2 in Fig. 1). Thus, superposition of two effects will result in a doublet UWB pulse as shown in Fig. 1.

The experimental setup is shown in Fig. 1. The pump, wavelength at 1557.1 nm, was modulated by an intensity modulator (IM) into super-Gaussian pulses (~ 105 ps pulse width). The self-edited pattern of single “1” in every 30 bits was used (0.32 GHz equivalent repetition rate). The pump was amplified to 13.6 dBm average power by an erbium-doped fiber amplifier

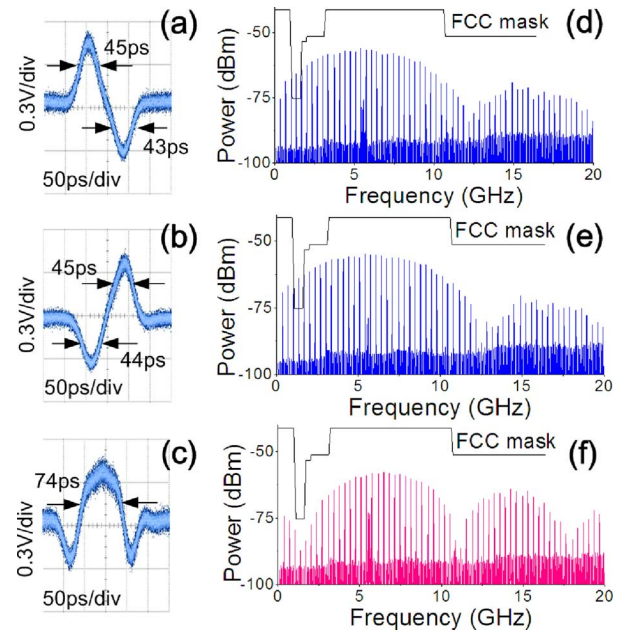


Fig. 2. (a)–(b) Monocycle and (c) doublet pulses and (d)–(f) the corresponding electrical spectra for back-to-back link.

(EDFA1), after which a 0.8 nm tunable bandpass filter (TBPF1) was inserted to reduce the amplified spontaneous emission (ASE) noise level from EDFA1. On the other branch, the CW probe light at 1540.02 nm was amplified to 12 dBm by EDFA2. The polarization controller (PC) after TBPF2 was used to align the state-of-polarization (SOP) of the probe with the pump. After coupling by a wavelength-division multiplexing coupler (WDMC), the two waves copropagated through a 400 m HNL-DSF ($\lambda_0 = 1554$ nm, $\gamma \approx 14$ W $^{-1}$ km $^{-1}$). The VBTBPF was set to the minimum bandwidth of 0.2 nm and centered at the probe wavelength. Such narrow bandwidth is critical to achieve PM-IM conversion, for which steep transmission function is crucial. The transmission link (arrow 1 in Fig. 1) consisted of a 25 km SMF with 4-km-matched dispersion-compensating fiber (DCF). A variable optical attenuator (VOA) in the back-to-back link (arrow 2 in Fig. 1) was used for comparison with the fiber transmission link at the same power level. At the receiver, after photodiodes (PDs), both a digital communication analyzer (DCA: Agilent 86100A, 20 GHz bandwidth) and an electrical spectrum analyzer (ESA: Agilent E4440A, bandwidth: 3 Hz to 26.5 GHz) were employed to measure the waveforms and spectra of the UWB pulses, respectively.

III. EXPERIMENTAL RESULTS AND DISCUSSION

The measured monocycle and doublet pulses and the corresponding electrical spectra are shown in Fig. 2. The full-width at half maximum (FWHM) of the monocycle in Fig. 2(a) and (b) are 45 ps. The asymmetry of the pulses was caused by over compensation of the residual OPA effect against the self-phase modulation (SPM) of the pump pulse comparing to [3], where SPM induced asymmetry was observed. The corresponding electrical spectra are shown in Fig. 2(d) and (e). While the doublet pulse is shown in Fig. 2(c) with 74 ps pulsewidth and spectrum shown in Fig. 2(f). The pulsewidth of the doublet pulse can be finely controlled by balancing the contribution of XPM and OPA, while only XPM is utilized in monocycle generation. The center frequencies are 5.4 GHz, 5.7 GHz and 6.4 GHz in Fig. 2(d)–(f), respectively. The

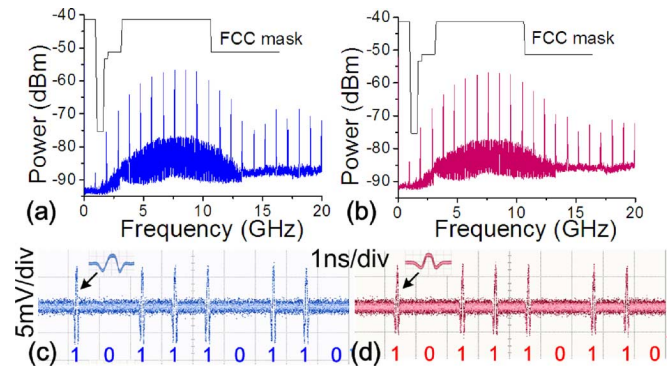


Fig. 3. Frequency spectra of the encoded UWB signal: (a) before and (b) after 25-km SMF at 950 Mb/s with a $2^7 - 1$ PRBS pattern. The waveforms: (c) before and (d) after the transmission, with a pattern of “101110110”.

corresponding 10-dB bandwidths are approximately 8.8 GHz, 9 GHz and 6.8 GHz, respectively. It is worthy to note that the spectrum of doublet pulses is much better suppressed at lower frequency around 1.575 GHz than those of monocycle pulses, which is crucial for noninterference operation with global positioning system (GPS) transmission in this spectrum region. Thus, in this case, using doublet-shape signals with optimized pulsewidth and shape will gain higher spectral efficiency.

To further evaluate the performance of our system, the encoded doublet signal was transmitted through 25 km SMF and 4-km-matched DCF, while the setup remained the same as previously presented. The UWB signal bits, “1” and “0” consisting of “1000000000” and “0000000000” following a $2^7 - 1$ pseudorandom bit sequence (PRBS) pattern, were transmitted at 950 Mb/s which was limited by the programmability of our pattern generator. It is also noted that other modulation formats like pulse-position modulation (PPM) and pulse shape modulation (PSM) could also be applicable in potential. While the average pump power was 1.76 dB higher to keep the OPA gain constant for both cases. The spectra of the signals in B2B and after the transmission are shown in Fig. 3(a) and (b), with the corresponding waveforms following the pattern of “101110110” shown in Fig. 3(c) and (d). Comparing Fig. 3(a) and (b), there is no observable change after the transmission. The center frequency is around 7.61 GHz with 10-dB bandwidth from 3.8 to 10.47 GHz, indicating $\sim 88\%$ fractional bandwidth in both Fig. 3(a) and (b). The enlarged pulses (insets of Fig. 3(c) and (d)) further prove that the pulse distortion is neglectable. Additionally, the UWB pulse distortion with 50% chromatic dispersion compensation was investigated, while the output electrical spectrum was still fully compliant with the FCC mask. However, to quantitatively evaluate the performance, the bit-error rate (BER) before and after the transmission should be calculated and compared with a high-speed digital sampling oscilloscope (DSO) [7]–[9]. Furthermore, air link will also be included to complete the evaluation of the entire UWB-over-fiber system. All these issues will be investigated in the next study phase.

IV. CONCLUSION

In conclusion, we have experimentally demonstrated a photonic UWB pulses generation scheme in a HNL-DSF

based phase and intensity modulator. Comparing to the pure phase modulation to intensity modulation (PM-IM) conversion scheme, our system, based on XPM and OPA, can achieve the enhanced wavelength tunability and pulse shaping flexibility, simultaneously. The encoded doublet signal, fully compliant with the FCC regulations, is transmitted at 950-Mb/s through a 25 km SMF while keeping the FCC indoor spectrum mask without any obvious pulse distortion. Furthermore, benefiting from the ultrafast dynamic response and wide gain bandwidth of OPA in the HNL-DSF, the proposed UWB-over-fiber communication system has potential in even higher speed operation and enhanced tunability to wider wavelength range.

REFERENCES

- [1] M. G. D. Benedetto, T. K. aiser, A. F. Molisch, I. Oppermann, C. Politano, and D. Porcino, *UWB Communication Systems: A Comprehensive Overview*. New York: Hindawi, 2004.
- [2] J. Yao, F. Zeng, and Q. Wang, “Photonic generation of ultrawideband signals,” *J. Lightw. Technol.*, vol. 25, no. 11, pp. 3219–3235, Nov. 2007.
- [3] F. Zeng, Q. Wang, and J. Yao, “All-optical UWB impulse generation based on cross-phase modulation and frequency discrimination,” *Electron. Lett.*, vol. 43, pp. 121–122, 2007.
- [4] Q. Wang, F. Zeng, S. Blais, and J. Yao, “Optical ultrawideband monocycle pulse generation based on cross-gain modulation in a semiconductor optical amplifier,” *Opt. Lett.*, vol. 31, pp. 3083–3085, 2006.
- [5] J. Dong, X. Zhang, J. Xu, D. Huang, S. Fu, and P. Shum, “Ultrawideband monocycle generation using cross-phase modulation in a semiconductor optical amplifier,” *Opt. Lett.*, vol. 32, pp. 1223–1225, 2007.
- [6] E. Zhou, X. Yu, X. Zhang, W. Xue, Y. Yu, J. Mørk, and I. T. Monroy, “Photonic generation of ultrawideband monocycle and doublet pulses by using a semiconductor-optical-amplifier-based wavelength converter,” *Opt. Lett.*, vol. 34, pp. 1336–1338, 2009.
- [7] T. B. Gibbon, X. Yu, D. Zibar, and I. T. Monroy, “Novel ultra-wideband photonic signal generation and transmission featuring digital signal processing bit error rate measurements,” in *Proc. OFC/NFOEC*, San Diego, CA, 2009, Paper OTuB8.
- [8] X. Yu, T. B. Gibbon, and I. T. Monroy, “Experimental demonstration of all-optical 781.25-Mb/s binary phase-coded UWB signal generation and transmission,” *IEEE Photon. Technol. Lett.*, vol. 21, no. 17, pp. 1235–1237, Sep. 1, 2009.
- [9] R. R. Lopez, A. Caballero, X. Yu, T. B. Gibbon, J. B. Jensen, and I. T. Monroy, “A comparison of electrical and photonic pulse generation for IR-UWB on fiber links,” *IEEE Photon. Technol. Lett.*, vol. 22, no. 5, pp. 263–265, Mar. 1, 2010.
- [10] Y. Dai and J. Yao, “Optical generation of binary phase-coded direct-sequence UWB signals using a multichannel chirped fiber bragg grating,” *J. Lightw. Technol.*, vol. 26, no. 15, pp. 2513–2520, Aug. 1, 2008.
- [11] S. Wang, H. Chen, M. Xin, M. Chen, and S. Xie, “Optical ultra-wideband pulse bipolar and shape modulation based on a symmetric PM-IM conversion architecture,” *Opt. Lett.*, vol. 34, pp. 3092–3094, 2009.
- [12] S. Pan and J. Yao, “A photonic UWB generator reconfigurable for multiple modulation formats,” *IEEE Photon. Technol. Lett.*, vol. 21, no. 19, pp. 1381–1383, Oct. 1, 2009.
- [13] M. Hanawa, K. Mori, K. Nakamura, A. Matsui, Y. Kanda, and K. Nonaka, “Dispersion tolerant UWB-IR-over-fiber transmission under FCC indoor spectrum mask,” in *Proc. OFC/NFOEC*, San Diego, CA, 2009, Paper OTuJ3.
- [14] J. Li, B. P. P. Kuo, and K. K. Y. Wong, “Ultra-wideband pulse generation based on cross-gain modulation in fiber optical parametric amplifier,” *IEEE Photon. Technol. Lett.*, vol. 21, no. 4, pp. 212–214, Feb. 15, 2009.
- [15] J. Li, Y. Liang, and K. K. Y. Wong, “Millimeter-wave UWB signal generation via frequency up-conversion using fiber optical parametric amplifier,” *IEEE Photon. Technol. Lett.*, vol. 21, no. 17, pp. 1172–1174, Sep. 1, 2009.
- [16] Y. Zhou, B. P. P. Kuo, K. K. Y. Cheung, S. Yang, P. C. Chui, and K. K. Y. Wong, “Wide-band generation of picosecond pulse using fiber optical parametric amplifier and oscillator,” *IEEE J. Quantum Electron.*, vol. 45, no. 11, pp. 1350–1356, Nov. 2009.